2018-09-14

Histone citrullination represses miRNA expression resulting in increased oncogene mRNAs in somatolactotrope cells.

Stanley B DeVore
University of Wyoming

Et al.

AMERICAN SOCIETY FOR MICROBIOLOGY | Molecular and Cellular Biology®

RESEARCH ARTICLE

Histone Citrullination Represses MicroRNA Expression, Resulting in Increased Oncogene mRNAs in Somatolactotrope Cells

Stanley B. DeVore,[a] Coleman H. Young,[a] Guangyuan Li,[a] Anitha Sundararajan,[b] Thiruvarangan Ramaraj,[b] Joann Mudge,[b] Faye Schilkey,[b] Aaron Muth,[c]* Paul R. Thompson,[c] Brian D. Cherrington[a]

[a]Department of Zoology and Physiology, University of Wyoming, Laramie, Wyoming, USA
[b]National Center for Genome Resources, Santa Fe, New Mexico, USA
[c]Department of Biochemistry and Molecular Pharmacology, University of Massachusetts Medical School, Worcester, Massachusetts, USA

ABSTRACT Peptidylarginine deiminase (PAD) enzymes convert histone arginine residues into citrulline to modulate chromatin organization and gene expression. Although PADs are expressed in anterior pituitary gland cells, their functional role and expression in pituitary adenomas are unknown. To begin to address these issues, we first examined normal human pituitaries and pituitary adenomas and found that PAD2, PAD4, and citrullinated histones are highest in prolactinomas and somatoprolactinomas. In the somatoprolactinoma-derived GH3 cell line, PADs citrullinate histone H3, which is attenuated by a pan-PAD inhibitor. RNA sequencing and chromatin immunoprecipitation (ChIP) studies show that the expression of microRNAs (miRNAs) let-7c-2, 23b, and 29c is suppressed by histone citrullination. Our studies demonstrate that these miRNAs directly target the mRNA of the oncogenes encoding HMGA, insulin-like growth factor 1 (IGF-1), and N-MYC, which are highly implicated in human prolactinoma/somatoprolactinoma pathogenesis. Our results are the first to define a direct role for PAD-catalyzed histone citrullination in miRNA expression, which may underlie the etiology of prolactinoma and somatoprolactinoma tumors through regulation of oncogene expression.

KEYWORDS citrullination, epigenetics, prolactinoma, miRNA, oncogenes

Many proteins are regulated by posttranslational modifications (PTMs) which alter their structure and function. One such modification is citrullination, or deimination, in which the basic amino acid arginine is converted to the neutral, noncoded residue citrulline (1). This modification is catalyzed by the peptidylarginine deiminase (PAD) family of enzymes composed of PAD1 to -4 and PAD6, although the last isoform lacks catalytic activity (2). In addition to cytosolic targets, PAD2 and PAD4 citrullinate nuclear proteins, such as histone tail arginine residues (3–5). Similar to acetylation and methylation, histone citrullination either activates or represses gene expression, thus contributing to the increasingly complex histone code (4, 6, 7). PADs are expressed in brain, skin, muscle, female reproductive tissues, and anterior pituitary gland lactotrope cells, suggesting a functional role for the enzymes *in vivo* (8–10).

The anterior pituitary gland contains five endocrine cell types, including lactotropes, which secrete prolactin (PRL), and somatotropes, which secrete growth hormone (GH). Somatolactotropes, a less understood, minor cell type, secrete both PRL and GH (11, 12). In humans and rodents, anterior pituitary cell populations can undergo dynamic changes in plasticity during different physiological states (13). Such transformations are critical for lactotrope cells, which dramatically increase in size, number, and connec-

Received 19 February 2018 **Returned for modification** 14 March 2018 **Accepted** 29 June 2018

Accepted manuscript posted online 9 July 2018

Citation DeVore SB, Young CH, Li G, Sundararajan A, Ramaraj T, Mudge J, Schilkey F, Muth A, Thompson PR, Cherrington BD. 2018. Histone citrullination represses microRNA expression, resulting in increased oncogene mRNAs in somatolactotrope cells. Mol Cell Biol 38:e00084-18. https://doi.org/10.1128/MCB.00084-18.

Address correspondence to Brian D. Cherrington, bcherrin@uwyo.edu.

* Present address: Aaron Muth, College of Pharmacy and Health Sciences, St. John's University, Queens, New York, USA.

tivity during late pregnancy to increase PRL production for the initiation of lactation (13–16). Yet uncontrolled proliferation can result in lactotrope-derived PRL-secreting prolactinomas, which account for 40 to 60% of all diagnosed functional pituitary adenomas (PAs) (17). Approximately 10 to 15% of PAs secrete GH, and the large majority of these are somatoprolactinomas, which secrete both GH and PRL (17, 18). A growing body of research implicates the overexpression of PADs in the pathogenesis of multiple cancers and in tumor progression (5, 19, 20). Currently, it is unknown if PAD-catalyzed histone citrullination alters gene expression in lactotrope cells or if it contributes to prolactinoma/somatoprolactinoma pathogenesis (21).

Genomic studies of human prolactinomas and somatoprolactinomas show that microRNA (miRNA) profiles differ between PA subtypes (22, 23). miRNAs are conserved 19- to 25-nucleotide (nt) noncoding RNAs that bind to complementary sequences within target mRNAs to regulate their expression (22, 24). miRNA biogenesis begins with transcription of a >200-nt primary miRNA (pri-miRNA) with a single miRNA or a cluster of miRNAs embedded within its stem-loop structure(s) (22). The microprocessor complex, a heterodimer of the RNase III enzyme Drosha and the double-stranded RNA binding protein DiGeorge syndrome chromosomal region 8 (DGCR8), excises the stem-loop, yielding a 60- to 100-nt precursor miRNA (pre-miRNA) (22, 25). Exportin-5 shuttles the pre-miRNA from nucleus to the cytoplasm, where the RNase III enzyme Dicer removes the terminal loop to generate the 19- to 25-nt duplex miRNA intermediate. The duplex is loaded into the RNA-induced silencing complex (RISC), which retains one strand and guides the mature miRNA to its binding site, commonly in a target mRNA's 3′ untranslated region (UTR). miRNA binding inhibits translation and/or promotes degradation of the mRNA transcript (22, 24, 25). Although miRNA expression is epigenetically regulated by methylation and acetylation, it is unknown if histone citrullination may likewise regulate miRNAs (25).

Bioinformatic analyses predict that more than 60% of human protein-coding genes contain one or more conserved miRNA binding sites in their 3′ UTRs, indicating that a majority of such genes are susceptible to miRNA regulation (26). Some miRNAs, known as tumor suppressor miRNAs, target the mRNA of oncogenes. For example, members of the *LET-7* family of miRNAs target Ras, Myc, and importantly, high-mobility-group AT-hook 1 and 2 (HMGA1 and HMGA2) mRNAs, which are implicated in prolactinoma and somatoprolactinoma pathogenesis (24, 27, 28). Therefore, it is not surprising that global miRNA suppression promotes cancer cell transformation and is associated with an increasing number of human neoplasias, including breast, lung, and thyroid cancers and both prolactinomas and somatoprolactinomas (23, 24, 29, 30).

Here we report that human prolactinomas and somatoprolactinomas express high levels of PAD2 and PAD4 and contain citrullinated histones. The rat somatoprolactinoma-derived GH3 cell line likewise expresses PAD2 and -4, which citrullinate histones to suppress the expression of the tumor suppressor miRNAs let-7c-2, 23b (miR-23b), and miR-29c. When histone citrullination is attenuated by the PAD inhibitor biphenyl-benzimidazole-Cl-amidine (BB-ClA) or when PAD2 is knocked down, the miRNAs are reexpressed and processed and subsequently target oncogene mRNAs. Specifically, these miRNAs target HMGA1, insulin-like growth factor 1 (IGF-1), and N-MYC. GH3 proliferation is significantly decreased following PAD inhibition compared to vehicle-treated controls. Our work is the first to show that histone citrullination directly represses the expression of tumor suppressor miRNAs, thus linking PADs to the overexpression of oncogenes in pituitary adenomas.

RESULTS

Human prolactinomas and somatoprolactinomas express elevated levels of PADs and citrullinated histones. PADs are expressed in the anterior pituitary gland, but whether levels of these enzymes change in PAs is currently unknown. Thus, we first examined if PAD2 and -4 are expressed in normal human pituitaries as well as human prolactinomas and somatoprolactinomas using immunohistochemistry (IHC). Normal tissue sections ($n = 8$ females and $n = 6$ males) were probed with anti-PAD2 or

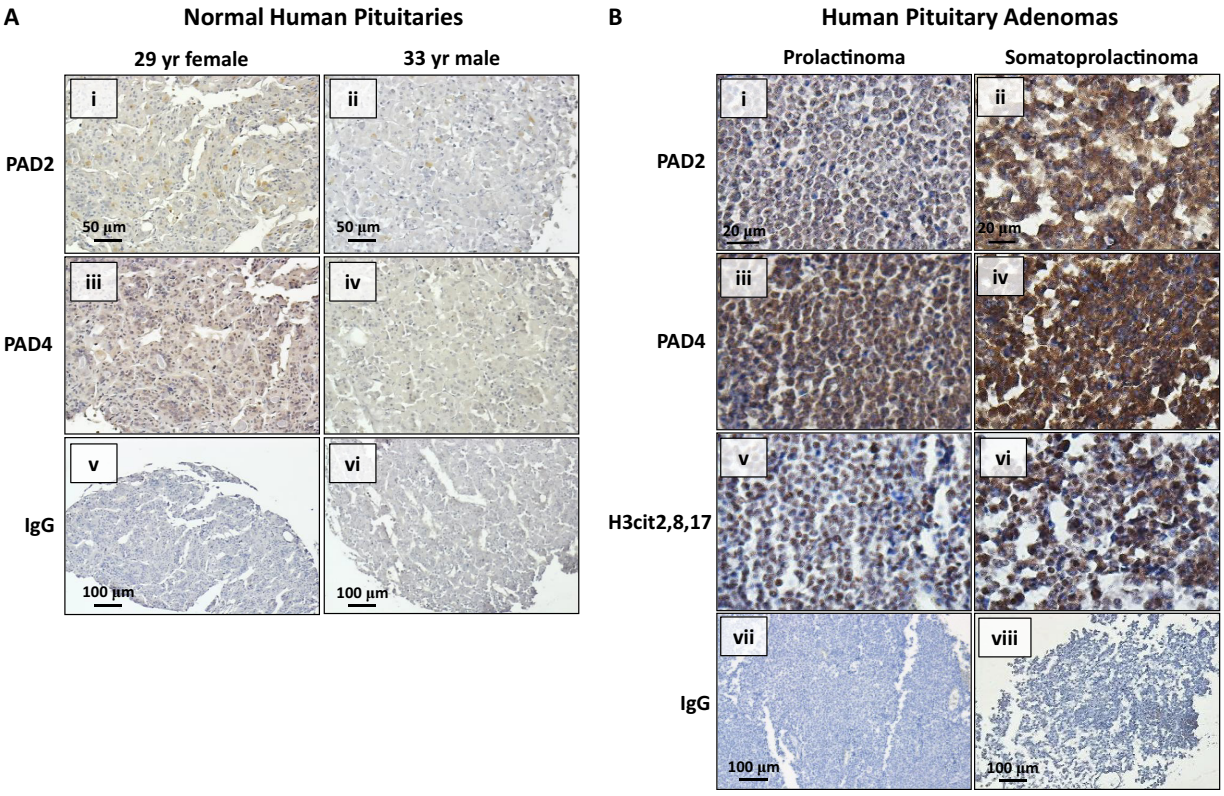

FIG 1 Human prolactinomas and somatoprolactinomas express elevated levels of PADs and citrullinated histones. (A) Normal human pituitary sections ($n = 8$ female and $n = 6$ male) were examined by IHC by probing with anti-PAD2 and anti-PAD4 antibodies or with an equal mass of rabbit IgG as a negative control. Representative images for a 29-year-old female and 33-year-old male were taken with a Zeiss Axio Vert.A1 microscope using the 20× objective except for IgG, which was taken with a 10× objective. (B) Human prolactinoma ($n = 11$) and somatoprolactinoma ($n = 6$) sections were examined by IHC using anti-PAD2, anti-PAD4, and anti-H3Cit2,8,17 antibodies. Sections were probed with an equal mass of rabbit IgG as a negative control. Representative images were taken using the 40× objective except for IgG, which was taken with a 10× objective. The scale bars represent 100 μm for the 10× objective, 50 μm for the 20× objective, and 20 μm for the 40× objective.

anti-PAD4 antibodies, while pituitary tumor sections ($n = 11$ prolactinoma and $n = 6$ somatoprolactinoma) were also probed with an anti-H3Cit2,8,17 antibody. Representative normal human female and male pituitary sections show little PAD2 (Fig. 1Ai and ii) or PAD4 (Fig. 1Aiii and iv) staining. Relative to the normal pituitary sections, an exemplar prolactinoma displays low PAD2 (Fig. 1Bi) and moderate PAD4 (Fig. 1Biii) staining; the somatoprolactinoma, however, has strong PAD2 (Fig. 1Bii) and PAD4 (Fig. 1Biv) expression. Consistent with elevated expression, PAD2 (Fig. 1Bi and ii) and PAD4 (Fig. 1Biii and iv) are localized to the nucleus and citrullinate histone H3 arginine residues 2, 8, and 17 (H3Cit2,8,17 [Fig. 1Bv and vi]). These findings illustrate that PADs and citrullinated histones are present in human prolactinomas and somatoprolactinomas at higher levels than in normal pituitaries.

PAD2 and PAD4 localize to the nucleus and citrullinate histones in the somatolactotrope-derived GH3 cell line. To address PAD function, we used the GH3 cell line derived from a female rat somatoprolactinoma (31). Consistent with somatolactotrope data from Fig. 1, GH3 lysates also express PAD2 and PAD4 (Fig. 2A). Cross-reactivity of the human PAD4 antibody with the rat isoform was assessed by preabsorbing with a rat N-terminal PAD4 15-amino-acid peptide, which significantly attenuates signal. To determine subcellular localization, GH3 cells were fixed and stained with anti-PAD2 or anti-PAD4 antibodies and IgG as a negative control following a standard immunocytochemistry (ICC) protocol. Confocal imaging confirmed the localization of both PAD isoforms in the cytoplasm and nuclei (Fig. 2B, arrows). The nuclear localization of PAD2 and PAD4 suggests that the enzymes may citrullinate histones in GH3 cells.

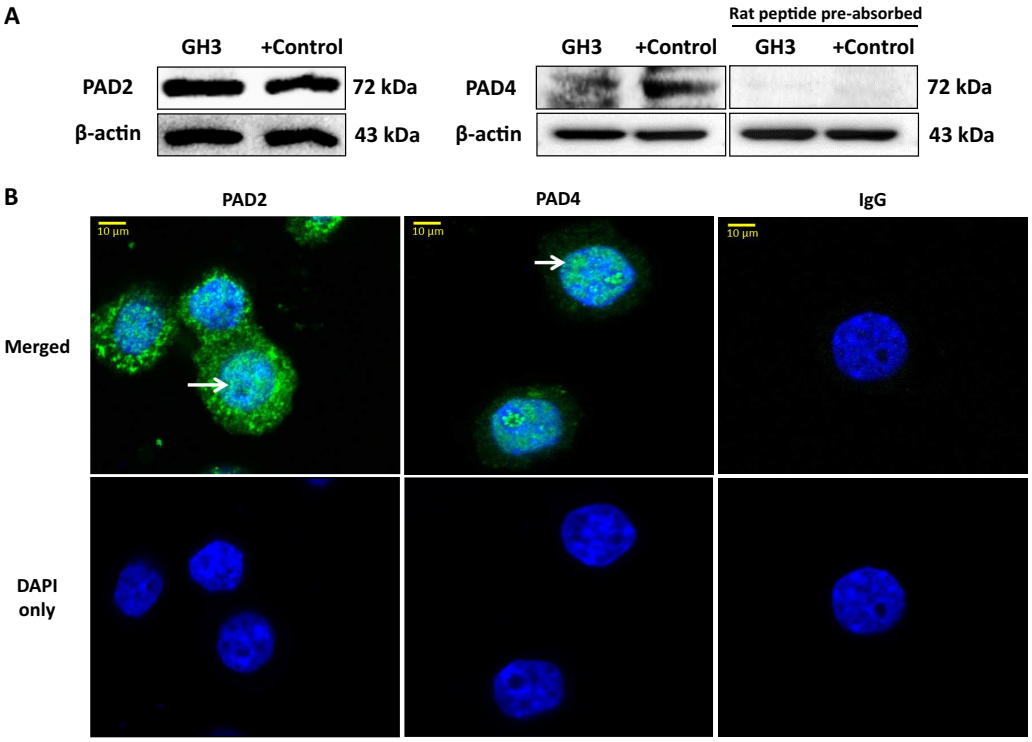

FIG 2 PAD2 and PAD4 localize to the nucleus and citrullinate histones in the somatolactotrope-derived GH3 cell line. (A) GH3 cells were lysed and subjected to Western blotting using anti-PAD2 and anti-PAD4 antibodies or an anti-PAD4 antibody that was preabsorbed with the N-terminal 15 amino acids of the rat PAD4 isoform. Anti-β-actin was used as a loading control. To generate positive controls, GH3 cells were transiently transfected with a PAD2 or PAD4 expression plasmid for 24 h and subsequently lysed. (B) GH3 cells were fixed and examined by ICC using anti-PAD2 or anti-PAD4 antibodies or an equal mass of rabbit IgG as a negative control and stained with 4′,6-diamidino-2-phenylindole (DAPI; blue). Arrows indicate nuclear PAD staining. Images were taken with a Zeiss LSM 710 confocal microscope using a 40× objective. The scale bars represent 10 μm.

To test this directly and confirm our results in Fig. 1B that show citrullinated histones in prolactinomas and somatoprolactinomas, GH3 cells were treated with either dimethyl sulfoxide (DMSO) or 1.25 μM BB-ClA every 3 h for a total of 14 h. Equal concentrations of purified histones were examined by Western blotting with *in vitro*-citrullinated histones as a positive control. Membranes were probed with an anti-H3Cit2,8,17 antibody or anti-histone H3 as a loading control. Our results indicate that GH3 cell histones are citrullinated under basal conditions, but PAD inhibition with BB-ClA treatment caused a significant ~50% decrease in histone H3 citrullination ($n = 3$; $P < 0.01$) (Fig. 3A and B). Thus, PADs catalyze the H3Cit2,8,17 epigenetic modification in GH3 cells, which is significantly inhibited by BB-ClA.

The pan-PAD inhibitor BB-ClA decreases basal histone citrullination to regulate the expression of pri-miRNAs in GH3 cells. Given that PADs citrullinate somatolactotrope histones, at issue is the identity of the genes epigenetically regulated by citrullination. To address this, we performed RNA sequencing (RNA-seq) on GH3 cells treated with either DMSO or 1.25 μM BB-ClA following the experimental paradigm described above. Total RNA from three independent experiments was collected and submitted for sequencing. Bioinformatic analysis found that inhibition of PAD-catalyzed citrullination significantly upregulated 81 genes and downregulates 74 genes. The top 12 upregulated genes are listed in Fig. 3C. Interestingly, PAD inhibition induced significant expression of multiple pri-miRNAs. Thus, it appears that PAD-catalyzed citrullination normally suppresses pri-miRNA expression. To the best of our knowledge, this is the first study showing that PAD-catalyzed citrullination directly regulates pri-miRNA expression.

Inhibiting histone citrullination or knocking down PAD2 increases the expression of primary microRNAs let-7c, 23b, and 29c. miRNAs are implicated in the

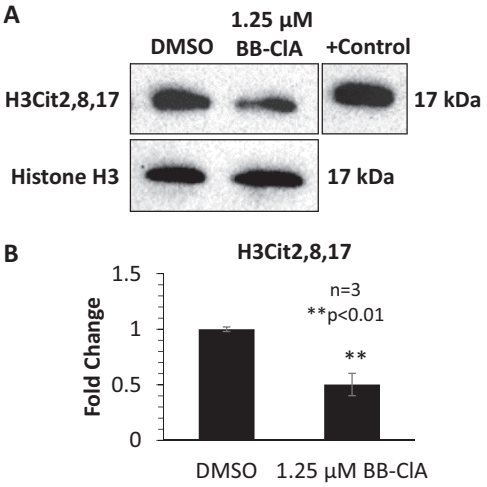

C

DMSO vs. 14hr 1.25 μM BB-ClA: Upregulated

SYMBOL	GENE NAME	FOLD CHANGE	P_{adj}
Hmox1	heme-oxygenase-1	5.985	1.56E-66
Mirlet7c-2	microRNA-let7c-2	3.500	2.75E-34
Npepo	aminopeptidase-O	2.901	4.79E-40
Dgcr8	DGCR8-microprocessor-complex-subunit	2.532	1.37E-32
Mir27b	microRNA-27b	2.392	2.38E-18
Mir3556b	microRNA-3556b	2.135	2.31E-10
Mir3074	microRNA-3074	2.075	5.77E-10
Mir1306	microRNA-1306	2.070	2.44E-09
Mir23b	microRNA-23b	1.981	2.99E-13
Mir29c	microRNA-29c	1.966	4.29E-09
Ftx	FTX-transcript-2C-XIST-regulator	1.826	4.35E-06
Lamp2	lysosomal-associated-membrane-protein-2	1.709	1.08E-04

FIG 3 The pan-PAD inhibitor BB-ClA decreases basal histone citrullination to regulate the expression of pri-miRNAs in GH3 cells. (A) GH3 cells were treated with either DMSO or 1.25 μM BB-ClA. Following cell lysis, histones were purified and examined by Western blotting using anti-H3Cit2,8,17 antibody and anti-histone H3 antibody as a loading control. *In vitro*-citrullinated histones were used as a positive control. (B) Western blots were quantified with Bio-Rad Image Lab; means were separated via a two-tailed *t* test ($n = 3$; $P < 0.01$), and values are expressed as means ± SEM. (C) GH3 cells were treated with either DMSO or 1.25 μM BB-ClA. The RNA from three independent experiments was purified and sequenced on an Illumina platform. Bioinformatic analysis identified 81 upregulated genes, of which the top 12 genes in DMSO- versus BB-ClA-treated GH3 cells are listed. Genes with P_{adj} values of <0.05 were considered significant.

etiology of prolactinomas and somatoprolactinomas (23, 29). Taken together with the data in Fig. 3, this suggests that PADs may be an unexplored mechanism through which pri-miRNA/miRNA expression promotes PAs. To confirm our RNA-seq results, we validated the expression of pri-let-7c-2, pri-miR-23b, and pri-miR-29c in GH3s since their respective mature miRNAs are associated with PAs and/or other human tumors (32–34). Following the same experimental paradigm, independent sets of RNA were isolated from GH3 cells and analyzed by qPCR using primers for pri-let-7c-2, pri-miR-23b, and pri-miR-29c. The primers detect only pri-miRNA transcripts since the forward primers are specific to regions that are removed during biogenesis. Our quantitative PCR (qPCR) results confirm a 2.5- to 4-fold increase in expression of each pri-miRNA transcript following PAD inhibition with BB-ClA ($n \geq 4$; $P < 0.001$) (Fig. 4A). We next examined the *in vivo* relevance of this finding using mouse pituitary primary cell cultures. Pituitaries from wild-type mice were explanted, dispersed, and plated in complete medium overnight. The following day, the cells were treated every 3 h for 14 total hours with DMSO or BB-ClA and pri-miRNA levels examined by qPCR. As with GH3 cells, pri-let-7c-2, pri-miR-23b, and pri-miR-29c expression was significantly increased upon PAD inhibition ($n \geq 4$; $P < 0.05$ and $P < 0.01$) (Fig. 4B). To confirm the results in Fig. 4A by another means, we next knocked down PAD2 and PAD4 in GH3 cells using small interfering RNAs (siRNAs). GH3 cells were transiently transfected with rat PAD2, PAD4, and nontargeting siRNAs for 48 h. Knockdown significantly decreased PAD2 and PAD4 expression compared to nontargeting controls ($n = 5$; $P < 0.05$ and $P < 0.01$) (Fig. 4C). siRNA-mediated knockdown of PAD2 but not PAD4 resulted in a significant increase in the expression of pri-let7c2, pri-miR-23b, and pri-miR-29c ($n \geq 4$; $P < 0.05$) (Fig. 4D to F).

Given the significant regulation that occurs at each step of miRNA biogenesis, we next quantified mature miRNA following PAD inhibition in GH3 cells. Our results indicate that mature miRNAs are also significantly increased with BB-ClA treatment compared to controls ($n = 4$; $P < 0.05$ and $P < 0.01$) (Fig. 4G) (25, 34). Finally, we used chromatin immunoprecipitation (ChIP) analysis to test if the changes in pri-miRNA expression are associated with histone citrullination of the miRNA genes. Following DMSO or BB-ClA treatment, GH3 cell lysates were incubated with the anti-H3Cit2,8,17 antibody and immunoprecipitated chromatin was analyzed by qPCR using primers specific to each pri-miRNA gene. The results indicate that significantly less of each

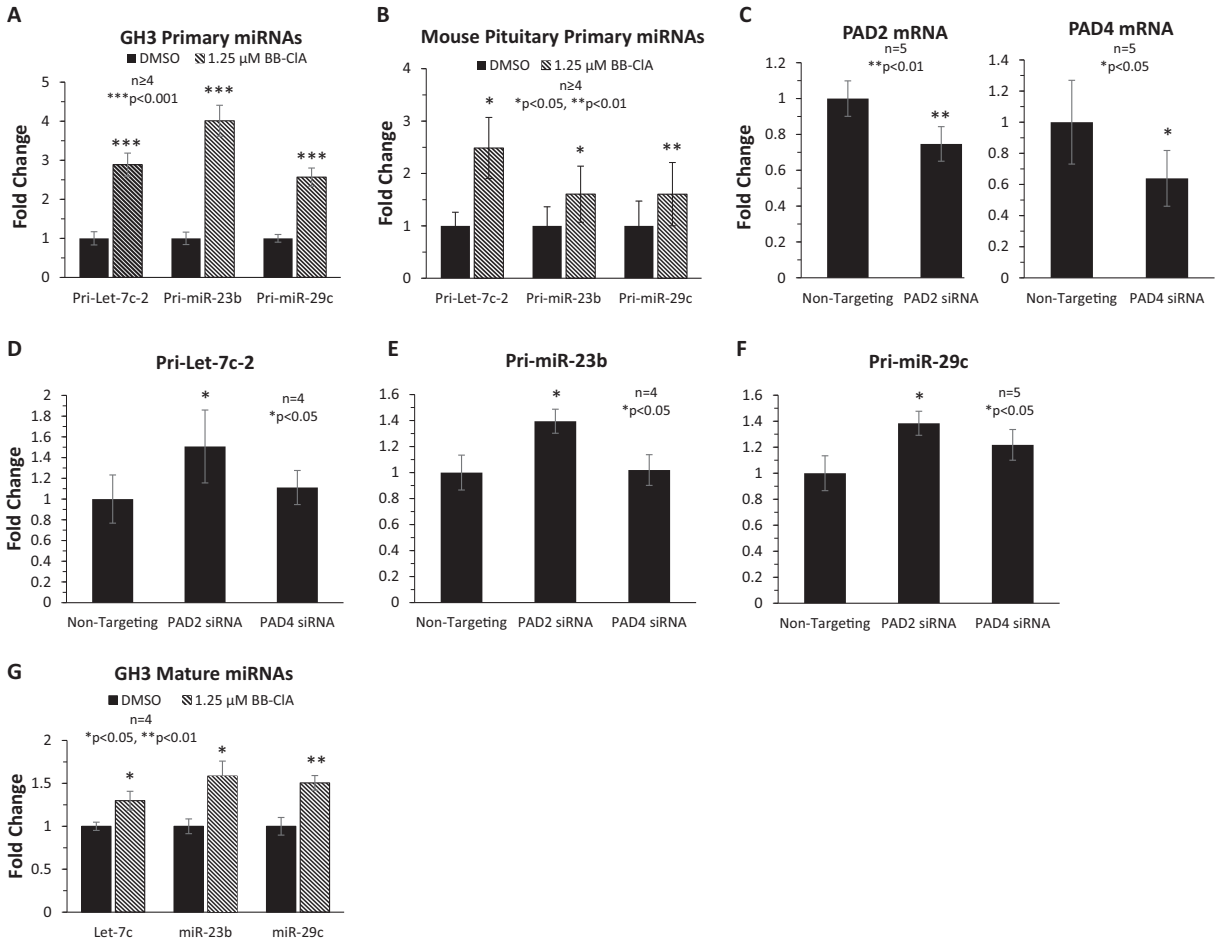

FIG 4 Inhibiting histone citrullination or knocking down PAD2 increases the expression of primary microRNAs let-7c, miR-23b, and miR-29c. (A) GH3 cells were treated with either DMSO or 1.25 μM BB-ClA and then lysed, and RNA was subjected to qPCR with primers specific to pri-let-7c-2, pri-miR-23b, and pri-miR-29c. Results were quantified ($n \geq 4$) and means were separated with a two-tailed *t* test. (B) Dispersed mouse pituitary cells were treated with either DMSO or 1.25 μM BB-ClA. Cells were lysed and purified RNA was subjected to qPCR with mouse primers for the indicated pri-miRNAs. Experiments were quantified ($n \geq 4$) and means were separated with a one-tailed paired *t* test. (C to F) GH3 cells were transiently transfected with nontargeting, PAD2, and PAD4 siRNA constructs for 48 h. Following lysis and RNA purification, samples were examined by qPCR for expression of PAD2 and -4 (C), pri-let7c-2 (D), pri-miR-23b (E), and pri-miR-29c (F), with GAPDH as the endogenous reference control. Means were separated with either a one-tailed paired *t* test (C; $n = 5$) or a one-way repeated-measures analysis of variance (ANOVA) with a *post hoc* Dunnett's *t* test (D to F; $n \geq 4$). (G) After DMSO or BB-ClA treatment, GH3 cells were lysed and purified small RNAs were subjected to qPCR with TaqMan probes specific for let-7c, miR-23b, and miR-29c. U6 snRNA was used as an endogenous reference control. Experiments were quantified and means were separated with a two-tailed *t* test ($n = 4$). All values provided are means ± SEM.

pri-miRNA gene is associated with citrullinated histones following PAD inhibition compared to vehicle-treated control cells ($n \geq 3$; $P < 0.05$) (Fig. 5). Thus, blocking PAD activity decreases H3Cit2,8,17 at the let-7c-2, miR-23b, and miR-29c genes. These data show that histone citrullination is repressive and directly suppresses the expression of these pri-miRNA genes.

PAD inhibition significantly decreases oncogene mRNA and protein expression in GH3 cells. HMGA1 and HMGA2 are nonhistone chromatin binding proteins that are directly implicated in the pathogenesis of prolactinomas and somatoprolactinomas (28, 35, 36). IGF-1 and N-MYC are similarly associated with oncogenic processes (37–40). TargetScan and visual analyses showed that the HMGA1, HMGA2, IGF-1, and N-MYC mRNAs contain putative binding sites for let-7 family members, miR-23b, and/or miR-29c (27, 32, 33). Given that histone citrullination suppresses pri-miRNA transcription, we hypothesized that inhibiting PADs in GH3 cells would decrease HMGA1, IGF-1, and N-MYC mRNAs due to the reexpression of miRNAs that promote transcript degradation. To test this, we examined HMGA1, IGF-1, and N-MYC mRNA levels after 0, 12, 24,

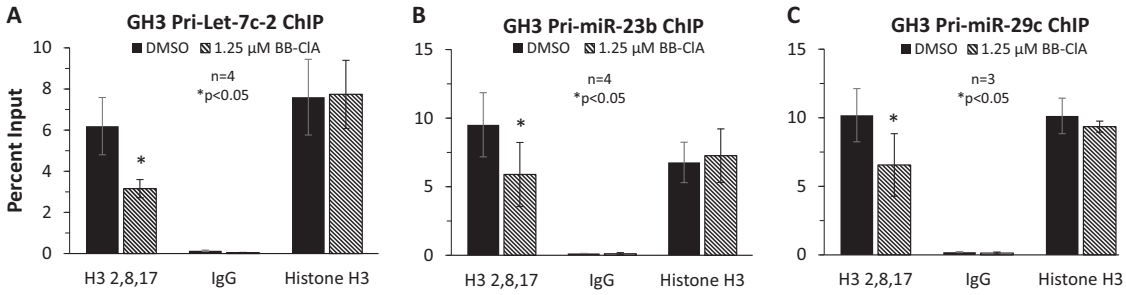

FIG 5 Citrullinated histones are directly associated with and repress primary miRNA expression in GH3 cells. For ChIP, GH3 protein-DNA complexes were immunoprecipitated with anti-H3Cit2,8,17, anti-histone H3 (positive control), or nonspecific IgG (negative control). Cross-links were reversed, and the DNA was purified and subjected to qPCR analysis with pri-miRNA specific primers. Means were separated with a one-tailed paired *t* test ($n \geq 3$). All values provided are means ± SEM.

and 48 h of treatment with 1.25 μM BB-ClA or DMSO with inhibitor replenishment every 12 h. HMGA2 was not analyzed due to lack of expression in GH3 cells (27). Our results indicate that HMGA1 and N-MYC mRNAs were significantly downregulated following 24 and 48 h of PAD inhibition, while IGF-1 mRNA was significantly decreased following 12, 24, and 48 h of BB-ClA (Fig. 6A to C) ($n \geq 3$; $P < 0.05$ and $P < 0.01$). HMGA1, N-MYC, and IGF-1 were also decreased following 48 h of BB-ClA treatment compared to DMSO-treated controls (Fig. 6D to F). Importantly, after 48 h of BB-ClA treatment

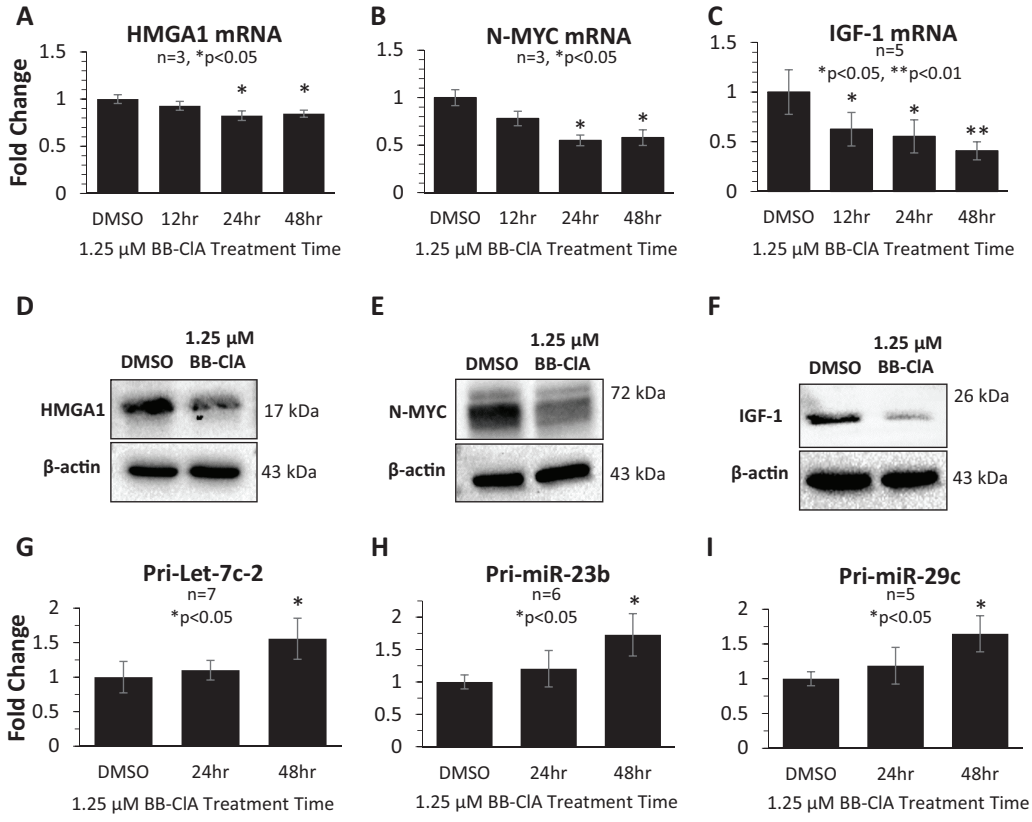

FIG 6 PAD inhibition significantly decreases oncogene mRNA and protein expression in GH3 cells. GH3 cells were treated every 12 h with 1.25 μM BB-ClA for 0, 12, 24, or 48 total hours. Following cell lysis, RNA was purified, reverse transcribed, and subjected to qPCR analysis using intron-spanning primers specific to HMGA1 (A), N-MYC (B), or IGF-1 (C). GAPDH was used as an endogenous reference control. Means were separated with a one-way repeated-measures ANOVA with a *post hoc* Dunnett's *t* test ($n \geq 3$). Following the same paradigm, HMGA1 (D), N-MYC (E), and IGF-1 (F) were examined by Western blotting. pri-let7c-2 (G), pri-miR-23b (H), and pri-miR-29c (I) expression was examined by qPCR after 24 and 48 h of BB-ClA treatment to confirm that pri-miRNAs were increased when oncogene expression was suppressed. Means were separated with a one-way repeated-measures ANOVA with a *post hoc* Dunnett's *t* test ($n \geq 5$). All values provided are means ± SEM.

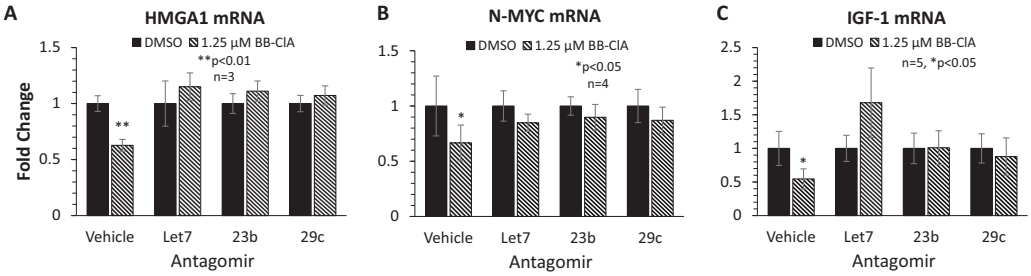

FIG 7 Antagomirs to let7c, miR-23b, and miR-29c attenuate oncogene mRNA expression in the presence of PAD inhibition. GH3 cells were transiently transfected with vehicle, let7c, miR-23b, and miR-29c antagomirs for 48 h. Immediately following transfection, cells were treated every 12 h with DMSO or 1.25 μM BB-ClA for 48 total hours. RNA was purified, reverse transcribed, and subjected to qPCR analysis using intron-spanning primers specific to HMGA1 (A), N-MYC (B), or IGF-1 (C). GAPDH was used as an endogenous reference control. Means were separated with a one-tailed paired *t* test. All values provided are means ± SEM.

pri-miRNAs let-7c-2, miR-23b, and miR-29c were significantly elevated compared to DMSO controls ($n \geq 5$; $P < 0.05$) (Fig. 6G to I). These data suggest that PAD inhibition promotes increased miRNAs that bind to target sequences within the HMGA1, IGF-1, and N-MYC mRNAs to decrease their expression.

Antagomirs to miRNAs let-7c-2, 23b, and 29c attenuate oncogene repression in the presence of PAD inhibition. Our results suggest that PADs may promote tumor proliferation by repressing miRNAs that target HMGA1, IGF-1, and N-MYC, thus allowing increased oncogene expression. Yet a direct relationship between let-7c-2, miR-23b, and miR-29c and oncogene mRNA expression in GH3 cells has not been shown. To address this, GH3 cells were transiently transfected for 48 h with antagomirs that specifically target let-7c-2, miR-23b, and miR-29c and simultaneously treated with DMSO or 1.25 μM BB-ClA every 12 h. qPCR analysis shows that similar to the results in Fig. 6A to C, HMGA1, IGF-1, and N-MYC mRNAs were significantly suppressed with BB-ClA treatment compared to those in DMSO-treated controls ($n \geq 3$; $P < 0.05$ and $P < 0.01$) (Fig. 7). Antagomirs for let-7c-2, miR-23b, and miR-29c all prevented a decrease in HMGA1, N-MYC, and IGF-1 mRNA expression in the presence of PAD inhibition by BB-ClA. Our results indicate that these PAD2-regulated miRNAs directly target the HMGA1, N-MYC, and IGF-1 mRNAs.

PAD inhibition attenuates GH3 proliferation. If histone citrullination indirectly elevates oncogenic mRNA, then it seems likely that this mechanism will increase proliferation rates of GH3 cells. To test this, we investigated if PAD inhibition alters GH3 cellular proliferation rates compared to those in vehicle-treated controls. Equal numbers of GH3 cells were treated every 12 h with 1.25 μM BB-ClA or DMSO for 24, 48, 72, or 96 total hours. At each time point, cellular proliferation was measured using a standard 3-(4,5-dimethyl-2-thiazolyl)-2,5-diphenyl-2H-tetrazolium bromide (MTT) proliferation assay. Our results show that PAD inhibition with BB-CLA significantly attenuated cellular proliferation relative to that in vehicle-treated controls at 72 and 96 h ($n = 3$; $P < 0.05$) (Fig. 8A). To corroborate these results, we also performed cell growth assays and quantified GH3 cells at 24, 48, 72, or 96 h following treatment with 1.25 μM BB-ClA or DMSO every 12 h. Similar to the MTT assay, results show that with 72 and 96 h of BB-ClA treatment there was a significant reduction in cell growth compared to that in DMSO-treated controls ($n = 5$; $P < 0.05$ and $P < 0.01$) (Fig. 8B). Cell viability was simultaneously measured using trypan blue exclusion, which found no significant difference between vehicle and BB-ClA treatment at 24, 48, or 72 h and a slight decrease in viability at 96 h ($n = 6$; $P < 0.01$) (Fig. 8C). These data are consistent with Fig. 4, which shows elevations in miRNAs, and Fig. 6, which demonstrates decreased oncogene mRNAs, and the data collectively indicate that PAD inhibition ultimately reduces GH3 proliferation.

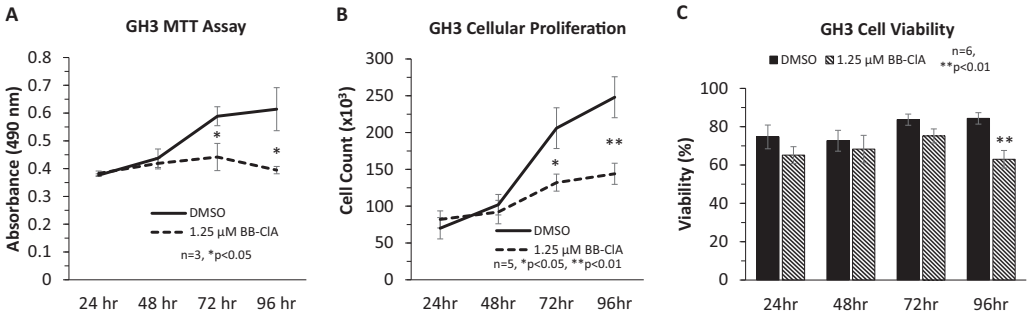

FIG 8 PAD inhibition attenuates GH3 proliferation. GH3 cells were treated every 12 h with DMSO or 1.25 μM BB-ClA for 24, 48, 72, or 96 total hours. (A) To quantify proliferation, the MTT tetrazolium reagent was added to each well. After 2 h, the resulting formazan solution was collected and the absorbance measured at 490 nm. Means were separated with one-tailed paired *t* tests ($n = 3$). (B and C) Cell growth (B) and viability (C) for DMSO and 1.25 μM BB-ClA treated GH3 cells were measured at 24, 48, 72, or 96 total hours using a Countess automated cell counter. Means were separated with one-tailed paired *t* tests ($n \geq 5$). All values provided are means ± SEM.

DISCUSSION

Our work defines a new role for PADs in epigenetic regulation of miRNA gene expression and shows that PAD2 and -4 and citrullinated histones are elevated in human prolactinomas and somatoprolactinomas. Mechanistically, PAD-catalyzed citrullination of H3Cit2,8,17 represses the expression of let-7c-2, miR-23b, and miR-29c. Without these tumor suppressor miRNAs, oncogenic HMGA1, N-MYC, and IGF-1 mRNAs increase resulting in cellular proliferation. Conversely, when PADs are inhibited or knocked down, tumor suppressor miRNAs are reexpressed and target oncogene mRNAs for repression and degradation, thereby suppressing proliferation (Fig. 9).

Compared to PAs, normal human pituitary tissues display low PAD2 and -4 staining. Our past work shows that PAD expression in female mouse pituitaries varies significantly across the estrous cycle and a similar trend in expression may occur in human pituitaries during the menstrual cycle (2, 21). Low expression in female pituitaries may simply reflect that the tissues were collected on a day of the menstrual cycle associated with low PAD expression. Low expression in normal human males is supported by previous studies of rodents which found that PAD expression is sexually dimorphic, with little expression in male pituitaries (10). Understanding the sexually dimorphic expression of PADs in pituitaries is the focus of ongoing investigations in our lab.

PAD inhibition results in a significant increase in expression of primary and mature let-7c, miR-23b, and miR-29c in GH3 cells and in pri-miRNAs in mouse pituitary cells compared to controls. Currently, BB-ClA is the most potent PAD inhibitor, yet it achieved only an approximately 50% reduction in histone citrullination (41). Despite this, elevated miRNAs following PAD inhibition are not unprecedented, as Cui et al.

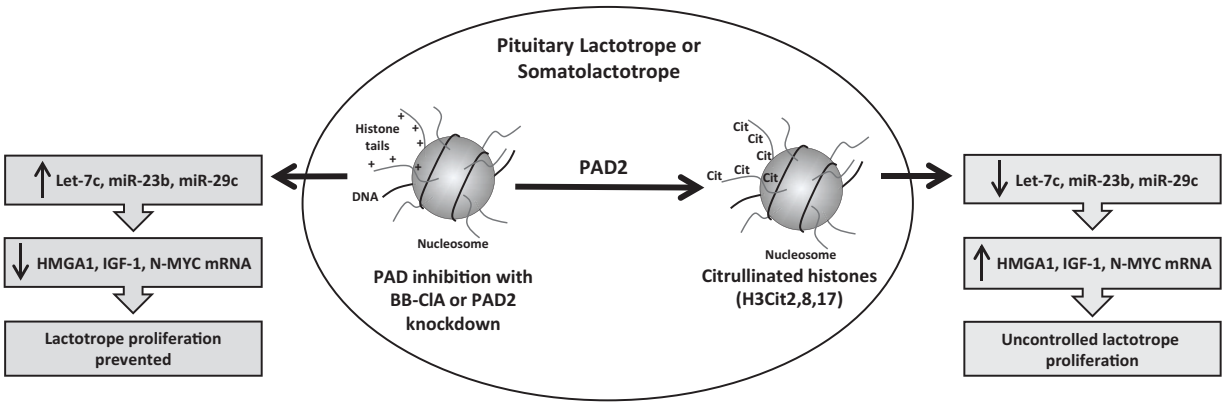

FIG 9 A working model for PAD catalyzed histone citrullination in lactotrope and somatolactotrope proliferation.

showed that the same mechanism is associated with the reexpression of miR-16 in colon cancer cells (42). Our ChIP studies are the first to show that histone citrullination is directly associated with the regulation of miRNA genes. In GH3 cells, the changes in mature miRNAs are not as robust as with pri-miRNAs, particularly with respect to let-7. This may occur because the let-7 TaqMan probe detects the mature miRNAs processed from both let-7c-1 and let-7c-2, while histone citrullination only controls the expression of the let-7c-2 isoform. Additionally, the fold changes in primary cell pri-miRNAs following BB-ClA treatment are lower than those from GH3 cells; however, this may be attributed to the heterogeneous cell population derived from the mouse pituitary gland.

Gene expression analyses have detected decreased let-7 miRNA in prolactinomas and somatoprolactinomas (23, 27, 32). let-7 miRNAs target and induce destabilization and subsequent degradation of oncogene mRNAs, including HMGA isoforms (24, 27, 28). Our findings suggest that aberrant PAD expression may increase histone citrullination, which suppresses let-7c expression, resulting in elevated oncoprotein levels. Although histone citrullination suppresses miR-23b expression in GH3 cells, Bottoni et al. showed that it is upregulated in human somatoprolactinomas (23). In contrast, Leone et al. observed significant downregulation of miR-23b in human somatotrope adenomas; however, it is unclear if these adenomas included GH/PRL-secreting somatoprolactinomas (33). Our studies are the first to show regulation of miR-29c in GH3 cells, although the clinical significance of this in PAs is unknown. An important implication from our work is that PAD-catalyzed histone citrullination is a plausible mechanism by which let-7c-2, miR-23b, and miR-29c are downregulated in PAs. Evidence of such epigenetic regulation of miRNA gene expression is not unprecedented (25). For example, DNA hypermethylation decreases let-7 and miR-23b expression and subsequently contributes to tumorigenesis (43, 44). In contrast, treatment of pituitary cells with the DNA methyltransferase inhibitor zebularine and the histone deacetylase inhibitor trichostatin A slows proliferation by inducing the reexpression of oncogene-targeting miRNAs (45). Our work shows that PAD-catalyzed histone citrullination represses tumor suppressor miRNA expression, which is potentially important in PA etiology.

PAD inhibition or knockdown facilitates increased miRNA expression, which results in a decrease in HMGA1, N-MYC, and IGF-1 mRNA. Our siRNA studies suggest that PAD2 is the predominant isoform that regulates pri-miRNA expression. Blocking miRNAs with antagomirs alleviates the BB-ClA-induced repression of HMGA1, N-MYC, and IGF-1 mRNA expression and demonstrates a direct relationship between the two. Interestingly, these target mRNAs are associated with the G_1/S cell cycle transition, and previous studies found that PAD inhibition or knockdown arrests cells at the same checkpoint (40, 42, 46–48). HMGA proteins modulate gene expression by altering chromatin architecture and are highly expressed in embryonic tissues, with minimal expression in adults (46). Reactivation of HMGA proteins in adult tissues is thought to promote tumorigenesis by displacing histone deacetylase 1 from the pRB/E2F-1 complex, which allows for the acetylation and activation of the proliferative effects of E2F-1 (67, 68). Furthermore, female transgenic mice overexpressing either HMGA1 or -2 almost exclusively develop GH/PRL-secreting somatoprolactinomas (35, 36). Previous work has demonstrated that let-7 targets the HMGA 3′ UTRs to promote transcript degradation (32). In agreement with our data, overexpression or upregulation of let-7 in GH3 cells decreases HMGA1 mRNA and attenuates cellular proliferation in a time-dependent manner (27, 32, 45). Our work suggests that miR-29c may also target HMGA-1 given that the antagomir to miR-29c prevents HMGA1 repression. IGF-1 is aberrantly expressed in prolactinomas of both human and diethylstibestrol (DES)-treated ACI rats, and abrogated IGF-1 signaling is strongly linked to the pathogenesis of many cancers (37, 38, 51). TargetScan and visual analyses identified several binding sites for let-7, miR-23b, and miR-29c within the IGF-1 mRNA sequence, and previous research showed that let-7 and miR-29c alter IGF-1 mRNA (52, 53). N-MYC is implicated in many cancers, and studies have characterized binding sites for let-7 and miR-29c

within N-MYC mRNA (40, 54, 55). It is important to point out that our RNA-seq data identified other miRNAs that are increased following PAD inhibition. Thus, we cannot rule out the possibility that the decrease in HMGA1, N-MYC, and IGF-1 mRNAs in GH3 cells following BB-ClA treatment was exclusively due to let-7c, miR-23b, or miR-29c. Although our RNA-seq data do not show a change in HMGA1, N-MYC, and IGF-1 expression following 14 h of BB-ClA treatment, we cannot eliminate the possibility that their genes are also regulated by histone citrullination at 48 h. Nonetheless, our studies suggest that PAD-mediated repression of tumor suppressor miRNAs promotes the overexpression of oncogenic proteins, which may contribute to the pathogenesis of prolactinomas and somatoprolactinomas.

In conclusion, we propose a model in which aberrant PAD expression and the resulting high levels of citrullinated histones act to suppress the expression of let-7c, miR-23b, and miR-29c, thereby allowing the reexpression of the HMGA1, N-MYC, and IGF-1 oncogenes, which drive cellular proliferation. These effects, however, can be prevented or reversed by knocking down PAD expression or blocking citrullination with the PAD inhibitor BB-ClA (Fig. 9). Studies to test whether inhibiting PAD activity *in vivo* alters oncogene mRNA profiles and cellular proliferation of primary lactotrope cells are under way. Although off-target effects are a legitimate concern, PAD inhibitors may represent novel therapeutic modalities for treatment of proliferation in the multiple cancers that overexpress PAD enzymes and contain citrullinated histones.

MATERIALS AND METHODS

Materials. The anti-PAD2 (12110-1-AP), IGF-1 (20215-1-AP), and N-Myc (10159-2-AP) antibodies were obtained from ProteinTech (Rosemont, IL), and the anti-PAD4 antibody (P4749) was from Sigma-Aldrich (St. Louis, MO). The anti-β-actin (Ab8227), anti-histone H3 (Ab1791), anti-H3Cit2,8,17 (Ab5103), and anti-HMGA1 (Ab129153) antibodies are from Abcam Inc. (Cambridge, MA). The let-7c-2-5p (IH-320289-05-0002), miR-23b-3p (IH-320310-05-0002), and miR-29c-3p (IH-320322-06-0002) antagomirs as well as the nontargeting (sense, UUCUCCGAACGUGUCACGU-dTdT; antisense, ACGUGACACGUUCGGAGAA-dTdT), PAD2 (sense, CCCGUUCUUUGGCCAGCGC-dTdT; antisense, GCGCUGGCCAAAGAACGGG-dTdT), and PAD4 (sense, GAAGGAUUUCCCUGUCAAA-dTdT; antisense, UUUGACAGGGAAAUCCUUC-dTdT) siRNAs were purchased from Dharmacon (Lafeyette, CO). The PAD inhibitor BB-ClA was generously provided by Paul R. Thompson (University of Massachusetts, Worcester, MA) and was synthesized as previously described (41). Rat PAD4 blocking peptide (MAQGAVIHVAPEEPT) was synthesized by and purchased from GenScript (Piscataway, NJ).

Cell culture and transient transfection. GH3 cells were obtained from Clay and Colorado State University and authenticated by treatment with E2 and quantification of c-myc and parvalbumin expression (56). GH3 cells were maintained as previously described (31). For the MTT assay, miRNA target qPCR, and antagomir studies, complete medium was used since longer exposure to BB-ClA was required. Complete medium was also necessary for primary culture experiments to allow cell survival. In remaining experiments, cells were plated and incubated before treatments in phenol red-free, charcoal-stripped fetal bovine serum (FBS) medium as previously described (56, 57). For PAD siRNA and antagomir transient-transfection studies, equal numbers of GH3 cells were plated and then transfected the following morning with 35 nM siRNAs or 30 nM antagomirs using DharmaFECT 1 (GE Healthcare, Chicago, IL) for 48 h according to manufacturer protocols. GH3 cells transfected with antagomirs were treated with DMSO or 1.25 μM BB-ClA every 12 h for 48 h.

IHC and immunocytochemistry (ICC). A normal human pituitary tissue array slide was obtained from US Biomax, Inc. (PIT501; Derwood, MD). Pituitary tumor samples and their subtype pathology were obtained from Institut D'Investigacions Biomediques August Pi i Sunyer Biobanc (Barcelona, Spain). Samples were deidentified and thus were exempt from University of Wyoming institutional review board (IRB) approval (protocol number 20140814BC00496). Immunohistochemistry (IHC) was performed as previously described (58, 59). Briefly, slides were incubated with anti-PAD2, -PAD4, or -H3Cit2,8,17 antibodies at 1:100 in 1× phosphate-buffered saline (PBS) overnight at 4°C, and negative-control slides were incubated with an equal mass of nonspecific rabbit IgG (Vector Laboratories). Images were taken with a Zeiss Axio Vert.A1 microscope using the 10×, 20×, and 40× objectives.

For ICC, GH3 cells were grown in MatTek 35-mm glass-bottom dishes (Ashland, MA). After being fixed and permeabilized, cells were incubated with primary antibodies (anti-PAD2, 1:100, or anti-PAD4, 1:100) overnight at 4°C. Duplicate dishes were incubated with an equal mass of nonspecific rabbit IgG as a negative control. Samples were imaged by a Zeiss LSM 710 confocal microscope under a 40× objective.

Western blotting. Positive controls for the anti-H3Cit2,8,17 antibody were generated by *in vitro* citrullination of bulk histones. For PAD2 and PAD4 antibody positive controls, GH3 cells were transiently transfected with PAD2 or PAD4 expression plasmids for 24 h following the Mirus Bio *Trans*IT-2020 (Madison, WI) transfection protocol. To determine the cross-reactivity of human PAD4 antibody with the rat PAD4 isoform, the antibody was diluted 1:1,000 in blocking buffer and then equally divided between two tubes. Rat PAD4 blocking peptide (400 μg/ml) was added to one tube and incubated overnight at 4°C with agitation. Samples of GH3 cell lysates and GH3 cells overexpressing human PAD4 were run side

by side on a 10% SDS-PAGE gel, and the membrane cut in half. Membranes were probed with the anti-PAD4 antibody or anti-PAD4 antibody preabsorbed with the rat blocking peptide.

For histone citrullination, GH3s were plated in 70-mm culture dishes and treated with 1.25 μM BB-ClA or dimethyl sulfoxide (DMSO) vehicle every 3 h for 14 total hours. Histones were purified as described by Shechter et al. (60). GH3 cells were lysed in radioimmunoprecipitation assay (RIPA) buffer and Western blotting was performed as previously described (49). Protein concentrations were determined by Pierce 660-nm protein assay for equal loading. Samples were then subjected to SDS-PAGE using 10% (PAD blots) or 15% gels (histone blots). Membranes were incubated overnight at 4°C with primary antibodies: anti-PAD2 (1:2,000), anti-PAD4 (1:1,000), anti-β-actin (1:5,000), anti-H3Cit2,8,17 (1:1,000) (0.9 μg/μl), anti-HMGA1 (1:10,000), anti-IGF-1 (1:500), anti-N-Myc (1:500), anti-histone H3 (1:5,000). Membranes were visualized on a Bio-Rad Chemidoc XRS using SuperSignal West Pico and Femto chemiluminescence substrate (Pierce, Rockford, IL). As loading controls, PAD blots were examined for β-actin, while citrullinated histone blots were probed for total histone H3. Results were quantified using Bio-Rad Image Lab software.

Quantitative PCR. RNA was purified following the Omega Bio-Tek E.Z.N.A. total RNA kit I protocol (Omega Bio-Tek, Inc., Norcross, GA). One microgram of the purified RNA was reverse transcribed using iScript reverse transcription (RT) supermix for RT-qPCR (Bio-Rad, Hercules, CA). cDNA was subjected to qPCR analysis using intron-spanning rat-specific primers (pri-let-7c-2, TAGGAGGGACCTCGAGAAGC [forward] and AAGGCCGTCAGTCAGTCTTG [reverse]; pri-miR-23b, CATGTGGATGGGAGTGGTT [forward] and CAAATCAGCATGCCAGGAA [reverse]; pri-miR-29c, AGGACTGCTTCATTCACATCAG [forward] and ACCAGG ACTGAGTGCTCCAC [reverse]; HMGA1, GTCAGAAGGAGCCCAGTGAA [forward] and CCCCGGAGTTGTGGT AACT [reverse]; IGF-1, ACTGACATGCCCAAGACTCA [forward] and TCCTTTGCAGCTTCCTTTTC [reverse]; N-Myc, GTGTCTGTCCCGGCTGTAG [forward] and TCCTCCTCATCGTCTTCATCA [reverse]; PAD2, TGGACCG ATGTCTACAGTGC [forward] and CACCCTCCGAGTGCTTCA [reverse]; PAD4, GCTGGGAAGGATCAGAGCAC [forward] and GGGAGTCTTCGTGCTTAGGG [reverse]; glyceraldehyde-3-phosphate dehydrogenase [GAPDH], CA ACTCCCTCAAGATTGTCAGCAA [forward] and GGCATGGACTGTGGTCATGA [reverse]). For mature miRNA analyses, cells were treated as described above but miRNAs were purified per the Omega Bio-Tek E.Z.N.A. miRNA kit (Omega Bio-Tek, Inc.) protocol. miRNAs were reverse transcribed using the TaqMan microRNA reverse transcription kit (Thermo Scientific) and small-RNA-specific stem-loop primers that were pooled according to Applied Biosystem's user bulletin PN 4465407 primer pool protocol. TaqMan probes for let7c-2-5p (assay identifier [ID] 000379, catalog no. 4427975), miR-23b-3p (0004000, 4427975), miR-29c-3p (000587, 4427975), and U6 snRNA (001973, 4427975) were purchased from Thermo Fisher. All qPCR data were analyzed using the threshold cycle ($2^{-\Delta\Delta CT}$) method using GAPDH for pri-miRNAs and mRNAs and U6 snRNA for mature miRNAs as reference genes (50).

Euthanasia and pituitary collection were performed in accordance with the guidelines outlined in the report of the AVMA on euthanasia (66). All work in this study was approved by the University of Wyoming Institutional Animal Care and Use Committee (protocol 20141104BC00129-02). For primary cell experiments, FVB wild-type mice were euthanized and pituitaries ($n = 7$) were explanted and dispersed as previously described (61). Cells were suspended in complete GH3 medium and the following morning treated with 1.25 μM BB-ClA or DMSO every 3 h for 14 total hours. RNA was purified, reverse transcribed, and analyzed by qPCR using mouse-specific primers (Pri-let-7c-2, TTCCTCTAGGAGGGACCTCAA [forward] and CGTCAGTCAGTCTTGGCGTA [reverse]; pri-miR-23b, TTGTCTCCCAGTCCCCTATG [forward] and GTGC AGCCTGCTGTCCTT [reverse]; pri-miR-29c, CAGACTGTCACCTGCCTTGA [forward] and GGAGAAATCGGTC AGCCTGT [reverse]; GAPDH, GGGTTCCTATAAATACGGACTGC [forward] and CCATTTTGTCTACGGGACGA [reverse]).

Illumina RNA sequencing. Three independent sets of GH3 cell RNA were generated as described above. RNA samples were sent to the National Center for Genomic Resources (NCGR; Santa Fe, NM). RNA libraries were prepared using the Illumina TruSeq library kit. A polyadenylation step during library preparation ensured retention of mRNA in the samples. Libraries were sequenced on HiSeq 2000 to generate 1 $\times$ 50 reads (single end reads). Adapters and primer sequences were removed during postprocessing.

Postprocessed high-quality reads for all samples were aligned to the *Rattus norvegicus* genome, downloaded from the GenBank repository (GCA_000001895.4). An associated annotation file in GFF format was used to obtain genic information to generate read counts. Alignments were generated using GSNAP (version released on 29 December 2014) using the following parameters: indel penalty = 2, maximum mismatches = 0.06, and everything else at default (62). Alpheus, an in-house pipeline, was used to generate reads (63). Gene expression for each sample was calculated as a measure of the total number of reads aligning uniquely to the reference, binned by genic coordinates (information obtained from the annotation file). Differential gene expression analysis was performed using the Bioconductor package DESeq2 (64). Raw read counts obtained were normalized to account for differences in sequencing depth and composition using methods implemented within DESeq2. Differential expression of pairwise comparisons was assessed using the negative binomial test, and comparisons that were significantly differentially expressed were defined as candidates that had an adjusted P value of $\leq$0.05 (65).

ChIP. GH3 cells were plated in 15-cm plates and treated as described above. Chromatin immunoprecipitation (ChIP) was then performed following the SimpleChip Plus enzymatic chromatin IP kit protocol (Cell Signaling Technologies, Danvers, MA), optimized for GH3 cells. The ChIP primer sequences were identical to the primer sets used for RT-qPCR. All values are expressed as percent input.

Cell proliferation, growth, and viability assays. GH3 cells were treated every 12 h with either DMSO or 1.25 μM BB-ClA. At 24, 48, 72, and 96 h, medium was removed from the corresponding wells

and replaced with 500 μl of complete medium and 20 μl of CellTiter 96 AQueous One solution reagent from the CellTiter 96 AQueous One cell proliferation assay (Promega Corporation, Madison, WI). After incubation for 2 h at 37°C, the absorbances of 100 μl were measured at 490 nm. For cell growth and viability, equal numbers of GH3 cells were seeded into 6-well plates and then treated with DMSO or 1.25 μM BB-ClA every 12 h. At 24, 48, 72, and 96 h, cells were counted and examined for viability using trypan blue following standard protocols for an Invitrogen Countess automated cell counter.

Statistics. All statistical analyses were performed with GraphPad Prism 6.0. Results were analyzed for significance using two-tailed *t* tests unless otherwise noted. All experiments were repeated at least three independent times. Values are given as means ± standard errors of the means (SEM).

Accession number(s). RNA sequencing data were deposited in the NCBI database with BioProject ID PRJNA422458.

ACKNOWLEDGMENTS

We thank Amy Navratil, Shaihla Khan and Jessica Berg for technical assistance in executing experiments.

This work was supported by the following grants: New Mexico INBRE Sequencing and Bioinformatics Core at NCGR through NIH/NIGMS P20GM103451, Wyoming INBRE Award NIH/NIGMS P20GM103432, University of Washington ITHS UL1TR000423, NIH/NICHD grant HD090541 to B.D.C., and NIH/NIGMS grant R35GM118112 to P.R.T.

REFERENCES

1. Vossenaar ER, Zendman AJW, van Venrooij WJ, Pruijn GJM. 2003. PAD, a growing family of citrullinating enzymes: genes, features and involvement in disease. Bioessays News Rev Mol Cell Dev Biol 25:1106–1118. https://doi.org/10.1002/bies.10357.
2. Horibata S, Coonrod SA, Cherrington BD. 2012. Role for peptidylarginine deiminase enzymes in disease and female reproduction. J Reprod Dev 58:274–282. https://doi.org/10.1262/jrd.2011-040.
3. Cuthbert GL, Daujat S, Snowden AW, Erdjument-Bromage H, Hagiwara T, Yamada M, Schneider R, Gregory PD, Tempst P, Bannister AJ, Kouzarides T. 2004. Histone deimination antagonizes arginine methylation. Cell 118:545–553. https://doi.org/10.1016/j.cell.2004.08.020.
4. Wang Y, Wysocka J, Sayegh J, Lee Y-H, Perlin JR, Leonelli L, Sonbuchner LS, McDonald CH, Cook RG, Dou Y, Roeder RG, Clarke S, Stallcup MR, Allis CD, Coonrod SA. 2004. Human PAD4 regulates histone arginine methylation levels via demethylimination. Science 306:279–283. https://doi.org/10.1126/science.1101400.
5. Cherrington BD, Zhang X, McElwee JL, Morency E, Anguish LJ, Coonrod SA. 2012. Potential role for PAD2 in gene regulation in breast cancer cells. PLoS One 7:e41242. https://doi.org/10.1371/journal.pone.0041242.
6. Jenuwein T, Allis CD. 2001. Translating the histone code. Science 293:1074–1080. https://doi.org/10.1126/science.1063127.
7. Zhang X, Bolt M, Guertin MJ, Chen W, Zhang S, Cherrington BD, Slade DJ, Dreyton CJ, Subramanian V, Bicker KL, Thompson PR, Mancini MA, Lis JT, Coonrod SA. 2012. Peptidylarginine deiminase 2-catalyzed histone H3 arginine 26 citrullination facilitates estrogen receptor α target gene activation. Proc Natl Acad Sci U S A 109:13331–13336. https://doi.org/10.1073/pnas.1203280109.
8. Akiyama K, Inoue K, Senshu T. 1989. Immunocytochemical study of peptidylarginine deiminase: localization of its immunoreactivity in prolactin cells of female rat pituitaries. Endocrinology 125:1121–1127. https://doi.org/10.1210/endo-125-3-1121.
9. Akiyama K, Nagata S, Tanaka S, Inoue K, Watanabe K, Senshu T. 1993. Search for functional significance of peptidylarginine deiminase in rat pituitaries: variation during pregnancy and ultrastructural localization in prolactin cells. Cell Biol Int 17:487–494. https://doi.org/10.1006/cbir.1993.1089.
10. Senshu T, Akiyama K, Nagata S, Watanabe K, Hikichi K. 1989. Peptidylarginine deiminase in rat pituitary: sex difference, estrous cycle-related changes, and estrogen dependence. Endocrinology 124:2666–2670. https://doi.org/10.1210/endo-124-6-2666.
11. Ooi GT, Tawadros N, Escalona RM. 2004. Pituitary cell lines and their endocrine applications. Mol Cell Endocrinol 228:1–21. https://doi.org/10.1016/j.mce.2004.07.018.
12. Yeung C-M, Chan C-B, Leung P-S, Cheng CHK. 2006. Cells of the anterior pituitary. Int J Biochem Cell Biol 38:1441–1449. https://doi.org/10.1016/j.biocel.2006.02.012.
13. Le Tissier PR, Hodson DJ, Martin AO, Romanò N, Mollard P. 2015. Plasticity of the prolactin (PRL) axis: mechanisms underlying regulation of output in female mice. Adv Exp Med Biol 846:139–162. https://doi.org/10.1007/978-3-319-12114-7_6.
14. Oishi Y, Okuda M, Takahashi H, Fujii T, Morii S. 1993. Cellular proliferation in the anterior pituitary gland of normal adult rats: influences of sex, estrous cycle, and circadian change. Anat Rec 235:111–120. https://doi.org/10.1002/ar.1092350111.
15. Melmed S. 2003. Mechanisms for pituitary tumorigenesis: the plastic pituitary. J Clin Invest 112:1603–1618. https://doi.org/10.1172/JCI20401.
16. Horvath E, Kovacs K, Scheithauer BW. 1999. Pituitary hyperplasia. Pituitary 1:169–179. https://doi.org/10.1023/A:1009952930425.
17. Seltzer J, Scotton TC, Kang K, Zada G, Carmichael JD. 2016. Gene expression in prolactinomas: a systematic review. Pituitary 19:93–104. https://doi.org/10.1007/s11102-015-0674-1.
18. Osamura RY, Kajiya H, Takei M, Egashira N, Tobita M, Takekoshi S, Teramoto A. 2008. Pathology of the human pituitary adenomas. Histochem Cell Biol 130:495–507. https://doi.org/10.1007/s00418-008-0472-1.
19. Wang L, Chang X, Yuan G, Zhao Y, Wang P. 2010. Expression of peptidylarginine deiminase type 4 in ovarian tumors. Int J Biol Sci 6:454–464. https://doi.org/10.7150/ijbs.6.454.
20. Wang S, Wang Y. 2013. Peptidylarginine deiminases in citrullination, gene regulation, health and pathogenesis. Biochim Biophys Acta 1829:1126–1135. https://doi.org/10.1016/j.bbagrm.2013.07.003.
21. Khan SA, Edwards BS, Muth A, Thompson PR, Cherrington BD, Navratil AM. 2016. GnRH stimulates peptidylarginine deiminase catalyzed histone citrullination in gonadotrope cells. Mol Endocrinol 30:1081–1091. https://doi.org/10.1210/me.2016-1085.
22. Gadelha MR, Kasuki L, Dénes J, Trivellin G, Korbonits M. 2013. MicroRNAs: suggested role in pituitary adenoma pathogenesis. J Endocrinol Invest 36:889–895. https://doi.org/10.1007/BF03346759.
23. Bottoni A, Zatelli MC, Ferracin M, Tagliati F, Piccin D, Vignali C, Calin GA, Negrini M, Croce CM, Degli Uberti EC. 2007. Identification of differentially expressed microRNAs by microarray: a possible role for microRNA genes in pituitary adenomas. J Cell Physiol 210:370–377. https://doi.org/10.1002/jcp.20832.
24. Roush S, Slack FJ. 2008. The let-7 family of microRNAs. Trends Cell Biol 18:505–516. https://doi.org/10.1016/j.tcb.2008.07.007.
25. Davis-Dusenbery BN, Hata A. 2010. Mechanisms of control of microRNA biogenesis. J Biochem 148:381–392.
26. Ha M, Kim VN. 2014. Regulation of microRNA biogenesis. Nat Rev Mol Cell Biol 15:509–524. https://doi.org/10.1038/nrm3838.
27. Palmieri D, D'Angelo D, Valentino T, De Martino I, Ferraro A, Wierinckx A, Fedele M, Trouillas J, Fusco A. 2012. Downregulation of HMGA-targeting microRNAs has a critical role in human pituitary tumorigenesis. Oncogene 31:3857–3865. https://doi.org/10.1038/onc.2011.557.
28. Fedele M, Palmieri D, Fusco A. 2010. HMGA2: a pituitary tumour subtype-specific oncogene? Mol Cell Endocrinol 326:19–24. https://doi.org/10.1016/j.mce.2010.03.019.

29. Kumar MS, Lu J, Mercer KL, Golub TR, Jacks T. 2007. Impaired microRNA processing enhances cellular transformation and tumorigenesis. Nat Genet 39:673–677. https://doi.org/10.1038/ng2003.
30. Palumbo T, Faucz FR, Azevedo M, Xekouki P, Iliopoulos D, Stratakis CA. 2013. Functional screen analysis reveals miR-26b and miR-128 as central regulators of pituitary somatomammotrophic tumor growth through activation of the PTEN-AKT pathway. Oncogene 32:1651–1659. https://doi.org/10.1038/onc.2012.190.
31. Tashjian AH, Yasumura Y, Levine L, Sato GH, Parker ML. 1968. Establishment of clonal strains of rat pituitary tumor cells that secrete growth hormone. Endocrinology 82:342–352. https://doi.org/10.1210/endo-82-2-342.
32. Qian ZR, Asa SL, Siomi H, Siomi MC, Yoshimoto K, Yamada S, Wang EL, Rahman MM, Inoue H, Itakura M, Kudo E, Sano T. 2009. Overexpression of HMGA2 relates to reduction of the let-7 and its relationship to clinicopathological features in pituitary adenomas. Mod Pathol 22:431–441. https://doi.org/10.1038/modpathol.2008.202.
33. Leone V, Langella C, D'Angelo D, Mussnich P, Wierinckx A, Terracciano L, Raverot G, Lachuer J, Rotondi S, Jaffrain-Rea M-L, Trouillas J, Fusco A. 2014. Mir-23b and miR-130b expression is downregulated in pituitary adenomas. Mol Cell Endocrinol 390:1–7. https://doi.org/10.1016/j.mce.2014.03.002.
34. Kriegel AJ, Liu Y, Fang Y, Ding X, Liang M. 2012. The miR-29 family: genomics, cell biology, and relevance to renal and cardiovascular injury. Physiol Genomics 44:237–244. https://doi.org/10.1152/physiolgenomics.00141.2011.
35. Fedele M, Battista S, Kenyon L, Baldassarre G, Fidanza V, Klein-Szanto AJP, Parlow AF, Visone R, Pierantoni GM, Outwater E, Santoro M, Croce CM, Fusco A. 2002. Overexpression of the HMGA2 gene in transgenic mice leads to the onset of pituitary adenomas. Oncogene 21:3190–3198. https://doi.org/10.1038/sj.onc.1205428.
36. Fedele M, Pentimalli F, Baldassarre G, Battista S, Klein-Szanto AJP, Kenyon L, Visone R, De Martino I, Ciarmiello A, Arra C, Viglietto G, Croce CM, Fusco A. 2005. Transgenic mice overexpressing the wild-type form of the HMGA1 gene develop mixed growth hormone/prolactin cell pituitary adenomas and natural killer cell lymphomas. Oncogene 24:3427–3435. https://doi.org/10.1038/sj.onc.1208501.
37. Grimberg A. 2003. Mechanisms by which IGF-I may promote cancer. Cancer Biol Ther 2:630–635. https://doi.org/10.4161/cbt.2.6.678.
38. Brahmkhatri VP, Prasanna C, Atreya HS. 2015. Insulin-like growth factor system in cancer: novel targeted therapies. BioMed Res Int 2015:538019. https://doi.org/10.1155/2015/538019.
39. Helland Å, Anglesio MS, George J, Cowin PA, Johnstone CN, House CM, Sheppard KE, Etemadmoghadam D, Melnyk N, Rustgi AK, Phillips WA, Johnsen H, Holm R, Kristensen GB, Birrer MJ, Australian Ovarian Cancer Study Group, Pearson RB, Børresen-Dale A-L, Huntsman DG, deFazio A, Creighton CJ, Smyth GK, Bowtell DDL. 2011. Deregulation of MYCN, LIN28B and LET7 in a molecular subtype of aggressive high-grade serous ovarian cancers. PLoS One 6:e18064. https://doi.org/10.1371/journal.pone.0018064.
40. Ruiz-Pérez MV, Henley AB, Arsenian-Henriksson M. 2017. The MYCN protein in health and disease. Genes 8(4):E113.
41. Knight JS, Subramanian V, O'Dell AA, Yalavarthi S, Zhao W, Smith CK, Hodgin JB, Thompson PR, Kaplan MJ. 2015. Peptidylarginine deiminase inhibition disrupts NET formation and protects against kidney, skin and vascular disease in lupus-prone MRL/lpr mice. Ann Rheum Dis 74:2199–2206. https://doi.org/10.1136/annrheumdis-2014-205365.
42. Cui X, Witalison EE, Chumanevich AP, Chumanevich AA, Poudyal D, Subramanian V, Schetter AJ, Harris CC, Thompson PR, Hofseth LJ. 2013. The induction of microRNA-16 in colon cancer cells by protein arginine deiminase inhibition causes a p53-dependent cell cycle arrest. PLoS One 8:e53791. https://doi.org/10.1371/journal.pone.0053791.
43. Wang X, Cao L, Wang Y, Wang X, Liu N, You Y. 2012. Regulation of let-7 and its target oncogenes. Oncol Lett 3:955–960. https://doi.org/10.3892/ol.2012.609.
44. Campos-Viguri GE, Jiménez-Wences H, Peralta-Zaragoza O, Torres-Altamirano G, Soto-Flores DG, Hernández-Sotelo D, Alarcón-Romero LDC, Jiménez-López MA, Illades-Aguiar B, Fernández-Tilapa G. 2015. miR-23b as a potential tumor suppressor and its regulation by DNA methylation in cervical cancer. Infect Agent Cancer 10:42.
45. Kitchen MO, Yacqub-Usman K, Emes RD, Richardson A, Clayton RN, Farrell WE. 2015. Epidrug mediated re-expression of miRNA targeting the HMGA transcripts in pituitary cells. Pituitary 18:674–684. https://doi.org/10.1007/s11102-014-0630-5.
46. D'Angelo D, Palmieri D, Mussnich P, Roche M, Wierinckx A, Raverot G, Fedele M, Croce CM, Trouillas J, Fusco A. 2012. Altered microRNA expression profile in human pituitary GH adenomas: down-regulation of miRNA targeting HMGA1, HMGA2, and E2F1. J Clin Endocrinol Metab 97:E1128–E1138. https://doi.org/10.1210/jc.2011-3482.
47. Mairet-Coello G, Tury A, DiCicco-Bloom E. 2009. Insulin-like growth factor-1 promotes G(1)/S cell cycle progression through bidirectional regulation of cyclins and cyclin-dependent kinase inhibitors via the phosphatidylinositol 3-kinase/Akt pathway in developing rat cerebral cortex. J Neurosci 29:775–788. https://doi.org/10.1523/JNEUROSCI.1700-08.2009.
48. Li P, Yao H, Zhang Z, Li M, Luo Y, Thompson PR, Gilmour DS, Wang Y. 2008. Regulation of p53 target gene expression by peptidylarginine deiminase 4. Mol Cell Biol 28:4745–4758. https://doi.org/10.1128/MCB.01747-07.
49. Li G, Hayward IN, Jenkins BR, Rothfuss HM, Young CH, Nevalainen MT, Muth A, Thompson PR, Navratil AM, Cherrington BD. 2016. Peptidylarginine deiminase 3 (PAD3) is upregulated by prolactin stimulation of CID-9 cells and expressed in the lactating mouse mammary gland. PLoS One 11:e0147503. https://doi.org/10.1371/journal.pone.0147503.
50. Livak KJ, Schmittgen TD. 2001. Analysis of relative gene expression data using real-time quantitative PCR and the 2(−delta delta C(T)) method. Methods 25:402–408. https://doi.org/10.1006/meth.2001.1262.
51. Tong Y, Zheng Y, Zhou J, Oyesiku NM, Koeffler HP, Melmed S. 2012. Genomic characterization of human and rat prolactinomas. Endocrinology 153:3679–3691. https://doi.org/10.1210/en.2012-1056.
52. Hu Y, Deng F, Song J, Lin J, Li X, Tang Y, Zhou J, Tang T, Zheng L. 2015. Evaluation of miR-29c inhibits endotheliocyte migration and angiogenesis of human endothelial cells by suppressing the insulin like growth factor 1. Am J Transl Res 7:489–501.
53. Mellios N, Woodson J, Garcia RI, Crawford B, Sharma J, Sheridan SD, Haggarty SJ, Sur M. 2014. β2-Adrenergic receptor agonist ameliorates phenotypes and corrects microRNA-mediated IGF1 deficits in a mouse model of Rett syndrome. Proc Natl Acad Sci U S A 111:9947–9952. https://doi.org/10.1073/pnas.1309426111.
54. Gan L, Xiu R, Ren P, Yue M, Su H, Guo G, Xiao D, Yu J, Jiang H, Liu H, Hu G, Qing G. 2016. Metabolic targeting of oncogene MYC by selective activation of the proton-coupled monocarboxylate family of transporters. Oncogene 35:3037–3048. https://doi.org/10.1038/onc.2015.360.
55. Molenaar JJ, Domingo-Fernández R, Ebus ME, Lindner S, Koster J, Drabek K, Mestdagh P, van Sluis P, Valentijn LJ, van Nes J, Broekmans M, Haneveld F, Volckmann R, Bray I, Heukamp L, Sprüssel A, Thor T, Kieckbusch K, Klein-Hitpass L, Fischer M, Vandesompele J, Schramm A, van Noesel MM, Varesio L, Speleman F, Eggert A, Stallings RL, Caron HN, Versteeg R, Schulte JH. 2012. LIN28B induces neuroblastoma and enhances MYCN levels via let-7 suppression. Nat Genet 44:1199–1206. https://doi.org/10.1038/ng.2436.
56. Fujimoto N, Igarashi K, Kanno J, Honda H, Inoue T. 2004. Identification of estrogen-responsive genes in the GH3 cell line by cDNA microarray analysis. J Steroid Biochem Mol Biol 91:121–129. https://doi.org/10.1016/j.jsbmb.2004.02.006.
57. Berthois Y, Katzenellenbogen JA, Katzenellenbogen BS. 1986. Phenol red in tissue culture media is a weak estrogen: implications concerning the study of estrogen-responsive cells in culture. Proc Natl Acad Sci U S A 83:2496–2500. https://doi.org/10.1073/pnas.83.8.2496.
58. Cherrington BD, Morency E, Struble AM, Coonrod SA, Wakshlag JJ. 2010. Potential role for peptidylarginine deiminase 2 (PAD2) in citrullination of canine mammary epithelial cell histones. PLoS One 5:e11768. https://doi.org/10.1371/journal.pone.0011768.
59. Young CH, Rothfuss HM, Gard PF, Muth A, Thompson PR, Ashley RL, Cherrington BD. 2017. Citrullination regulates the expression of insulin-like growth factor-binding protein 1 (IGFBP1) in ovine uterine luminal epithelial cells. Reproduction 153:1–10. https://doi.org/10.1530/REP-16-0494.
60. Shechter D, Dormann HL, Allis CD, Hake SB. 2007. Extraction, purification and analysis of histones. Nat Protoc 2:1445–1457. https://doi.org/10.1038/nprot.2007.202.
61. Navratil AM, Knoll JG, Whitesell JD, Tobet SA, Clay CM. 2007. Neuroendocrine plasticity in the anterior pituitary: gonadotropin-releasing hormone-mediated movement in vitro and in vivo. Endocrinology 148:1736–1744. https://doi.org/10.1210/en.2006-1153.
62. Wu TD, Nacu S. 2010. Fast and SNP-tolerant detection of complex variants and splicing in short reads. Bioinformatics 26:873–881. https://doi.org/10.1093/bioinformatics/btq057.
63. Miller NA, Kingsmore SF, Farmer A, Langley RJ, Mudge J, Crow JA,

Gonzalez AJ, Schilkey FD, Kim RJ, van Velkinburgh J, May GD, Black CF, Myers MK, Utsey JP, Frost NS, Sugarbaker DJ, Bueno R, Gullans SR, Baxter SM, Day SW, Retzel EF. 2008. Management of high-throughput DNA sequencing projects: Alpheus. J Comput Sci Syst Biol 1:132.
64. Love MI, Huber W, Anders S. 2014. Moderated estimation of fold change and dispersion for RNA-seq data with DESeq2. Genome Biol 15:550. https://doi.org/10.1186/s13059-014-0550-8.
65. Hochberg Y, Benjamini Y. 1990. More powerful procedures for multiple significance testing. Stat Med 9:811–818. https://doi.org/10.1002/sim.4780090710.
66. American Veterinary Medical Association. 2013. AVMA guidelines for the euthanasia of animals: 2013 edition. American Veterinary Medical Association, Schaumburg, IL.
67. D'Angelo D, Esposito F, Fusco A. 2015. Epigenetic mechanisms leading to overexpression of HMGA proteins in human pituitary adenomas. Front Med 2:39.
68. Ueda Y, Watanabe S, Tei S, Saitoh N, Kuratsu J-I, Nakao M. 2007. High mobility group protein HMGA1 inhibits retinoblastoma protein-mediated cellular G0 arrest. Cancer Sci 98:1893–1901. https://doi.org/10.1111/j.1349-7006.2007.00608.x.